(4)

Technical Document 1717
December 1989

Transfer Matrices for Multimode Optical Fiber Systems

C. J. Gabriel

NAVAL OCEAN SYSTEMS CENTER

San Diego, California 92152-5000

J. D. FONTANA, CAPT, USN
Commander

R. M. HILLYER
Technical Director

ADMINISTRATIVE INFORMATION

This work was performed by the Optical Electronics Branch, Code 562, Naval Ocean Systems Center, for the David Taylor Research Center, Bethesda, Maryland.

Released by
M. N. McLandrich, Head
Optical Electronics Branch

Under authority of
H. E. Rast, Head
Electronic Material
Sciences Division

JG

CONTENTS

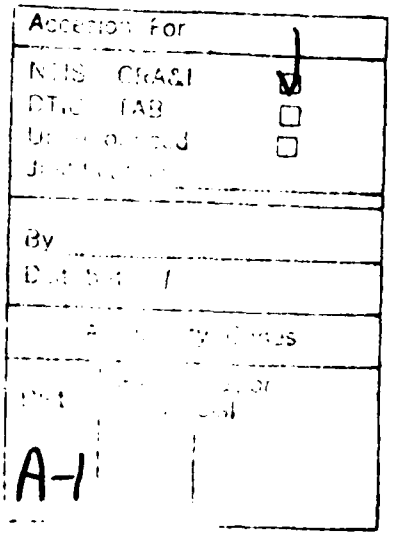

INTRODUCTION

Multimode fibers are used in short-haul, medium bit-rate applications where their large core diameters and numerical apertures permit the use of light-emitting diodes as sources to realize cost-effective optical systems. These fibers can guide several hundred modes and achieve bandwidth-length products of a few gigahertz-kilometer (references 1, 2, 3, and 4).

Because fiber-optical systems are not perfectly straight, uniformly cylindrical waveguides, optical power launched in a particular propagating mode does not necessarily remain in that mode. Not only is the optical power scattered into nonpropagating modes and ultimately lost to the system, but it is scattered between propagating modes as it flows through the components of the system. The characterization of this power flow is greatly complicated by the fact that different modes experience different group propagation delay and attenuation through each segment of the system. Consequently, details of the modification of the distribution of optical power among the propagating modes by a component are important in determining the optical performance of any subsequent fiber-optical component in the system. This dependency is known as the concatenation effect and should be considered in the specification, design, and maintenance of multimode-fiber-optical systems.

In this report, a transfer-matrix formalism for expressing the effect of a component on the mode-power distribution is discussed. It is expected that this formalism will serve to both clarify and extend matrix approaches to the description of this effect that have been presented by others and will ultimately result in component loss characterization methods that are independent of the launch conditions chosen to make the characterization (references 5, 6, 7, 8, 9, 10, 11, 12, and 13).

BASIC CONCEPTS

The mode-power distribution vector $\bar{u}$ specifies the power propagating in each mode and is designated by an azimuthal and radial mode-number pair. Consequently, a component can be characterized by a matrix of scattering coefficients $s_{ij,kl}$ giving the scattering of power in each possible mode u_{kl} at the input into every possible mode u'_{ij} at the output. For simplicity, it is assumed that all modes propagate in the same direction in the system, that is, reflected power is considered lost. The effect of a component on the power flow can then be written as the matrix product

$$u'_{i,j} = \sum_{k=1}^{K} \sum_{l=1}^{L} s_{ij,kl}\, u_{kl} \qquad (1)$$

where $i = 1,\ldots,I$ and $j = 1,\ldots,J$, in which there are $I \times J$ possible modes at the output and $K \times L$ possible modes at the input.

Because there are so many possible modes, the scattering matrix, s, cannot be practically used to characterize a component. Instead, a reduced-dimension-transfer matrix must be formed from s. Let T be a transformation from the K × L valued mode-power distribution, to an M valued reduced-dimension mode-power distribution. That is, define

$$p_m = \sum_{k=1}^{K} \sum_{l=1}^{L} T_{m,kl}\, u_{kl} \tag{2}$$

where m = 1,...,M, and $\bar{p}$ similarly in terms of T′ and $\bar{u}'$ so that

$$p'_m = \sum_{m=1}^{M} M_{nm}\, p_m \tag{3}$$

in which,

$$M_{nm} = \sum_{i=1}^{I} \sum_{j=1}^{U} \sum_{k=1}^{K} \sum_{l=1}^{L} T'_{n,ij}\, s_{ij,kl}\, T^{+}_{kl,m} \tag{4}$$

defines the reduced-dimension mode-power-transfer matrix. In this definition, the transformation $T^{+}_{kl,m}$ is the inverse of $T_{m,kl}$ in some best-possible sense, that is, so that $\bar{p}'$ obtained from equation 3 approximates $T'\bar{u}'$ if $\bar{p}$ is given by equation 2. Here, the Moore-Penrose generalized inverse (see appendix A) will be assumed.

Consider, as an example of dimension reduction, the transformation from the full radial/azimuthal mode description to the reduced-dimension fundamental-mode-number description in which the LP modes are grouped according to a fundamental mode number m = 2l-1+k (references 1, 14, and 15). While the actual form of the transformation needed to accomplish this reduction in dimension is not necessarily specified, evidently there is very

little error incurred in its use. Therefore, it must hold, in the appropriate sense (appendix A), that

$$\sum_{i=1}^{I} \sum_{j=1}^{J} T_{n,ij}\, T'_{ij,m} = \delta_{nm} \tag{5}$$

as well as

$$\sum_{m=1}^{M} T^{+}_{ij,m}\, T_{m,kl} = \delta_{ij}\, \delta_{jl} \tag{6}$$

where δ_{ij} is the Kronecker delta. In what follows, it will be assumed that the fundamental mode groups of the linearly polarized modes form the basis for further reduction in dimension. This is appropriate for loss characterization because while these modes may not be strongly coupled within a group (references 16 and 17), they appear to be essentially monotonic with respect to loss, that is, higher order modes are generally more attenuated than lower order modes.

MODE-BLOCK REDUCTION

An explicit example of a transformation, T, that combines fundamental-mode groups into mode blocks is the matrix

$$\begin{vmatrix} 1\ 1\ldots1\ 0\ 0\ldots0\ 0\ 0\ldots0\ldots0\ 0\ldots0 \\ 0\ 0\ldots0\ 1\ 1\ldots1\ 0\ 0\ldots0\ldots0\ 0\ldots0 \\ \qquad\qquad\qquad\quad \ldots \\ 0\ 0\ldots0\ 0\ 0\ldots0\ 0\ 0\ldots0\ldots1\ 1\ldots1 \end{vmatrix} \tag{7}$$

where there are M rows, one for each block and N columns, one for each fundamental-mode group, and, if the partition of the mode groups is N_m in the mth mode block, the number of ones in the diagonal non-zero partition of the mth row of T will be N_m. Here,

the modes are all weighted either zero or one. By inspection, the generalized inverse of this transformation, T^+, is

$$\begin{vmatrix} 1/N_1 & 0 & \dots & 0 \\ 1/N_1 & 0 & \dots & 0 \\ & \dots & & \\ 1/N_1 & 0 & \dots & 0 \\ 0 & 1/N_2 & \dots & 0 \\ 0 & 1/N_2 & \dots & 0 \\ & \dots & & \\ 0 & 1/N_2 & \dots & 0 \\ 0 & 0 & \dots & 0 \\ 0 & 0 & \dots & 0 \\ & \dots & & \\ 0 & 0 & \dots & 0 \\ 0 & 0 & \dots & 1/N_M \\ 0 & 0 & \dots & 1/N_M \\ & \dots & & \\ 0 & 0 & \dots & 1/N_M \end{vmatrix} \tag{8}$$

where there are N rows and M columns, in which there are N_m non-zero elements in the diagonal partition mth column.

The product TT^+ is the M by M identity matrix

$$\begin{vmatrix} 1 & 0 & \dots & 0 \\ 0 & 1 & \dots & 0 \\ & & \dots & \\ 0 & 0 & \dots & 1 \end{vmatrix} \tag{9}$$

while the product T^+T is the N by N matrix

$$\begin{vmatrix} E_1/N_1 & 0 & \dots & 0 \\ 0 & E_2/N_2 & \dots & 0 \\ & \dots & & \\ 0 & 0 & \dots & E_M/N_M \end{vmatrix} \tag{10}$$

in which E_m is the N_m by N_m matrix of all ones

$$\begin{vmatrix} 1 & 1 & \dots & 1 \\ 1 & 1 & \dots & 1 \\ & & \dots & \\ 1 & 1 & \dots & 1 \end{vmatrix} \tag{11}$$

Clearly, T^+ satisfies the conditions to be the unique generalized inverse of T and is, in the Frobinius norm, the matrix that makes T^+T closest to the N by N identity matrix (see appendix A).

A generalization of mode-block reduction is to choose T so that

$$\sum_{n=1}^{N} w_n T_{in} T_{jn} = \delta_{ij} \tag{12}$$

with i,j=1,...,M. Consequently,

$$T^{+}_{kl} = w_l T_{lk} \tag{13}$$

with l,k=1,...,N. In this instance, TT^{+} is again the M by M identity matrix, and the N by N matrix $T^{+}T$ with elements

$$(T^{+}T)_{ij} = \sum_{M=1}^{M} w_m T_{mi} T_{mj} \tag{14}$$

is in general not the identity matrix unless M = N. This extension amounts to taking the rows of T to be the first M polynomials from an N dimensional set of discrete orthogonal polynomials having a weight function w_n.

These examples illustrate the result that when the reduced-dimension transfer matrix for a concatenation of two components is expressed in terms of the individual components in the form

$$M^{12} = M^2 M^1 \tag{15}$$

which, by equation 4, can be rewritten as

$$M^{12} = T''s^2 T'^{+} T' s^1 T^{+} \tag{16}$$

it is not identical to the reduced-dimension transfer matrix for the same system that would be formed directly from the product of the two scattering matrices s^2s^1 because of the presence of the product $T'^{+}T'$, which, in general, is not an identity matrix. Consequently, some error must always be expected if a system is described in terms of the reduced-dimension transfer matrices of

its components; however, the error will be minimal in the Frobinius norm if T^+ is taken to be the Moore-Penrose generalized inverse of T (see appendix A).

CONTINUOUS MODE-POWER DISTRIBUTION

Measurement considerations prohibit the determination of even the fundamental-mode-number distribution so that further simplification of the mode distribution must be introduced. If the propagating field intensity is axially symmetric and the spectral width of the source $\delta\lambda$ satisfies a minimum width requirement, which for a parabolic index profile is

$$\frac{\delta\lambda}{\lambda} > \frac{\sqrt{2\Delta}}{a\ k\ n_{gw}} \tag{17}$$

where λ is the free-space wavelength, k is the free-space wave number, Δ is the relative-refractive-index difference, a is the core radius, and n_{gw} is the effective-group index of refraction, there will be many modes excited and they will be spaced more closely than their spectral width. In this situation, the mode-power distribution can be taken to be a continuous function of a continuous mode parameter rather than a discrete function of a discrete mode index (references 15 and 16). More important here, there exists a relationship between the continuous approximation to the mode-power distribution and the measurable near-field pattern, $I(\rho)$, on the end face of a fiber (references 16, 18, 19, 20, 21, 22, 23, and 24). This relationship takes

different forms depending on the choice of mode parameter, so some consideration of the mode parameter is necessary.

In the continuous approximation, it can be written that the total power propagating W is

$$W = \sum_{n=1}^{N} p_n = N \int_0^1 p_z(z)dz \tag{18}$$

where p_n is the optical power in the nth fundamental-mode group, N is the number of such mode groups, and $p_z(z)$ is the continuous approximation to the discrete distribution p_n. Here, z is the continuous extension of the discrete parameter n normalized so that $0 \leq z \leq 1$ and chosen so that the modes have a uniform density distribution N. Other choices for the continuous mode parameter, for example, $x:z=g(x)$, where $g(0) = 0$ and $g(1) = 1$ so that $0 \leq x \leq 1$, yield the generalization

$$W = \int_0^1 \sigma_x(x)\ p_x(x)\ dx \tag{19}$$

where

$$p_x(x) = p_z[g(x)] \tag{20}$$

and

$$g(x) = \frac{1}{N} \int_0^x \sigma_x(x)dx \tag{21}$$

in which

$$N = \int_0^1 \sigma_x(x)dx \quad . \tag{22}$$

We shall call $p_x(x)$ the $\sigma_x(x)$-density distribution corresponding to the continuous mode parameter $x=g^{-1}(z)$. These transformed descriptions of the mode distribution are all equivalent; furthermore, even though the uniform density distribution seems to

have a more natural physical interpretation in terms of the discrete mode distribution, it is not the most useful because the connection between a continuous mode-power distribution and the emittance, $I(\rho)$, on the face of the fiber has not been cast in terms of the uniform-density distribution.

The relationship between $I(\rho)$ and $p_x(x)$ shall be written here, neglecting leaky modes, as

$$I(s) = \frac{V^2}{2\pi a^2} \int_{f(s)}^{1} p_x(x)dx \qquad , s = \rho/a \tag{23}$$

where V is the normalized frequency, f(s) is the index of refraction profile tacitly assumed here to be monotonic, and ρ is the radial coordinate at the end face of the fiber. The normalized frequency can be written

$$V = a\ k\ n(0)\ \sqrt{2\Delta} \tag{24}$$

where n(0) is index of refraction at the center of the fiber core and the index of refraction profile is defined by

$$n^2(s) = n^2(0)\ [1 - 2\Delta f(s)] \tag{25}$$

and the condition that $0 \leq f(s) \leq 1$.

By differentiating both sides of equation 23, an explicit expression for $p_x(x)$ is obtained

$$I'(s) = -\frac{V^2}{2\pi a^2}\ p_x[f(s)]f'(s) \quad . \tag{26}$$

This expression is the one generally used to determine the mode-power distribution from measurements of the near-field pattern (references 8, 18, 23, and 24). Because equation 26 involves the ratio of the derivatives of the two quantities I(s)

and f(s) to determine $p_x(x)$, the presence of noise or distortion in the measurements of these quantities can introduce a large uncertainty into $p_x(x)$ particularly near extrema in f(s). An alternative method using equation 23 directly will be presented later in the section on experimental determination.

Another frequently occurring form for the relationship between the $I(\rho)$ and the mode distribution uses the parameter $y=\sqrt{x}$ (references 12, 16, and 25). For this change of variable, equation 23 yields

$$I(s) = \frac{V^2}{\pi a^2} \int_{\sqrt{f(s)}}^{1} y\, p_y(y)\, dy \tag{27}$$

and equation 26 takes the form

$$I'(s) = - \frac{V^2}{2\pi a^2} p_y\, [\sqrt{f(s)}]\, f'(s) \quad . \tag{28}$$

That neither x nor y is the uniform density parameter z can be seen from the total power flow in the fiber, which can be written in the case of x, for example, either as

$$W = 2\pi a^2 \int_0^1 s\, I(s)\, ds \tag{29}$$

or, by introducing equation 23 and changing the order of the s and x integration, as

$$W = \frac{V^2}{2} \int_0^1 [f^{-1}(x)]^2\, p_x\, dx \tag{30}$$

from which it can be seen that the mode density corresponding to the parameter x is

$$\sigma_x(s) = \frac{V^2}{2} [f^{-1}(x)]^2 \quad . \tag{31}$$

A more general example that is useful for computational purposes is that of the power profile where $f(s) = s^{\alpha}$ and $g(y) = y^{\beta}$. In this case,

$$I(s) = \frac{\beta V^2}{2\pi a^2} \int_{s^{\alpha/\beta}}^{1} y^{\beta-1} p_y(y)\, dy \tag{32}$$

and

$$\sigma_y(y) = \frac{\beta V^2}{2} y^{\beta(1+2/\alpha)-1} \quad . \tag{33}$$

Now it is seen that if β is chosen to have the value $\beta = \alpha/(\alpha+2)$, then we have the uniform-density choice of the mode parameter, that is, $y = z$ with the uniform mode density

$$\sigma_z = \frac{V^2 \alpha}{2(\alpha+2)} \tag{34}$$

being the number of propagating modes N. The near-field pattern is then given by

$$I(s) = \frac{V^2 \alpha}{2\pi a^2 (\alpha+2)} \int_{s^{\alpha+2}}^{1} z^{-2/(\alpha+2)} p_z(z)\, dz \quad . \tag{35}$$

Consequently, we obtain for the uniform-density mode-power distribution

$$p_z(z) = - \frac{2\pi a^2}{V^2 \alpha} z^{(1-\alpha)/(2+\alpha)} I'(s) \Big|_{s = z^{1/(\alpha+2)}} \quad . \tag{36}$$

The factor that appears in front of the integral in equation 23 may take different forms depending on the choice of units of $p_x(x)$, which need not be power per mode as we have selected. See equation 19, where $\sigma_x(x)$ has the units of modes per unit

continuum-mode parameter. For example, choosing units of radiance, that is, W/cm^2sr places quite a different physical interpretation on $p_x(x)$, but nevertheless results in a density function $\sigma_x(x)$ having a squared dependence on the inverse profile function just as in equation 31 (references 1 and 20). As will become evident later, the essential feature of equation 23 is that it is a linear relationship between I(s) and $p_x(x)$.

MATRIX FORMALISM FOR THE CONTINUOUS MODE DISTRIBUTION

Just as in the discrete case, a matrix formalism related to the measurable near-field patterns can now be introduced by assuming there exists a linear relationship of the form

$$p'_z(z) = \int_0^1 p_z(z')h_z(z',z)\,dz' \qquad (37)$$

where the primed and unprimed p designate, respectively, the output and input mode-power distributions of the element, and the kernel h(z',z) is a system response function that gives, essentially, the fraction of the power propagating in the region dz' about z' scattered into the region dz about z.

A matrix representation of h(z',z) is obtained by expanding $p'_z(z)$ and $p_z(z')$ in a suitable set of orthogonal functions $\{\phi_n(z)\}$, where

$$\int_0^1 w(z)\,\phi_i(z)\,\phi_j(z)\,dz = \delta_{ij} \qquad (38)$$

δ_{ij} is the Kronecker delta, and w(z) is the weight function of the set $\{\phi_m(z)\}$. Thus,

$$p_z(z') = \sum_{m=1}^{\infty} c_m \phi_m(z') \tag{39}$$

$$p_z(z) = \sum_{m=1}^{\infty} c'_m \phi_m(z) \quad . \tag{40}$$

Substituting equations 39 and 40 into equation 37, multiplying both sides of the result by $w(z)\,\phi_r(z)$, and integrating over z yields upon application of equation 38

$$c'_r = \sum_{m=1}^{\infty} H_{r,m} c_m, \quad r = 1,2,\ldots \tag{41}$$

where

$$H_{r,m} = \int_0^1 w(z)\phi_r(z)\left[\int_0^1 \phi_m(z')h(z',z)dz'\right]dz \tag{42}$$

are the elements of the desired matrix representation of h(z',z). Practically, the summations in equations 39 and 40 will have to be truncated at some term N with the results that H will be an N by N matrix approximation to h(z',z) and $\bar{c}'$ and $\bar{c}$ will be N by 1 matrix (vector) approximations to $p'_z(z)$ and $p_z(z)$, respectively. In matrix notation, equation 41 becomes

$$\bar{c}' = H\,\bar{c} \quad . \tag{43}$$

While the optical source can be represented by the vector $\bar{c}$, the representation of the photodetector requires the additional assumption that the signal current j can be obtained by a simple weighting of the mode-power distribution at the input of the photodetector. Thus,

$$j = N \int_0^1 p_z(z)\, R_z(z)\, dz \tag{44}$$

where, now

$$R_z(z) = \frac{w(z)}{N} \sum_{m=1}^{\infty} r_m \phi_m(z) \tag{45}$$

yielding upon application of equation 38

$$j = \sum_{m=1}^{\infty} r_m c_m \tag{46}$$

where the r_m are the vector coefficients of the photodetector response function $R_z(z)$. This expansion must be truncated, so $\bar{r}$ becomes a 1 by N matrix (vector) and the scalar photocurrent j can be approximated as the dot product

$$j = \bar{r} \cdot \bar{c} \quad . \tag{47}$$

Using a relationship such as equation 43, equation 47 can be rewritten as

$$j = \bar{r} \cdot H \bar{c} \quad . \tag{48}$$

This is the basic system equation in the transfer-matrix formalism and accounts for the mode-power distribution of the source, $\bar{c}$, the intermode scattering in the optical system, H, and the selective response of the photodetector, $\bar{r}$.

The details of the form chosen for equation 44 are unimportant for our purposes, and an equation like equation 47 could have been derived from consideration of the discrete formalism as well.

EXPERIMENTAL DETERMINATION

Neither equation 4 nor 42 is of much use other than to provide a theoretical background because neither the matrix $s_{ij,kl}$ nor the continuum function $h(z',z)$ appearing in them are likely to be obtainable. An exception to this might occur in situations where classes of components, such as lengths of fiber, can be

parametrized with only a few parameters resulting in significant simplification in the required measurements (references 26 and 27). Therefore, H must be determined directly from a set of input and output radiometric measurements from which input and output distributions $p_x(x)$ can be found. In the mode-continuum approximation, equation 26 provides such a needed relationship between the mode distribution and measurable near-field patterns. To avoid the numerical problems involved with evaluating derivatives of noisy data, as well as possible distortion-induced singularities, the integral form, equation 23, can be used in a least-square approach as follows.

Begin by expanding the mode-power distribution in a finite series

$$p_x(x) = \sum_{m=1}^{P} c_m \phi_m(x) \tag{49}$$

where P is small compared to the number of propagating modes, but must be equal to or larger than N, the dimension of the desired transfer matrix, and $\{\phi_m(x)\}$ is a suitable set of orthogonal functions. Now, in addition to errors produced by noise in the measured quantities, there will be an error caused by the truncation of the expansion at N. It is possible that the truncation error could be reduced if a rational function were used rather than a series expansion; however, here we are not interested in merely finding the mode-power distribution $p_x(x)$, but in obtaining a vector representation of it (refernce 28). Therefore, in order to reduce the effects of all errors, the c_n

are chosen to minimize the mean-square error in the power flow defined by

$$E^2 = 2\pi a^2 \int_0^1 s \left[I(s) - \frac{V^2}{2\pi a^2} \sum_{m=1}^{p} c_m \int_{f(s)}^{1} \phi_m(x)\,dx \right]^2 ds \quad . \qquad (50)$$

The normal equations for the c_n are obtained from

$$\frac{\partial E^2}{\partial c_r} = 0 \qquad r = 1, 2, \ldots, p \qquad (51)$$

which can be written in matrix form

$$A\,\bar{c} = \bar{b} \qquad (52)$$

where

$$A_{ij} = \int_0^1 s\ \psi_i(s)\ \psi_j(s)\ ds \qquad i,j = 1, \ldots, p \qquad (53)$$

$$b_j = \int_0^1 s\ I(s)\ \psi_j(s)\ ds \qquad j = 1, \ldots, p \qquad (54)$$

and

$$\psi_n(s) = \frac{V^2}{2\pi a^2} \int_{f(s)}^{1} \phi_n(x)\,dx \qquad , n = 1, \ldots, p \quad . \qquad (55)$$

The c_n obtained from the solution of the normal equations can be used directly to represent the reduced dimension mode-power distribution simply by truncating the vectors after N components, or the further reduction in dimension can be obtained by a subsequent transformation. For example, to obtain the N components p_j for a mode-block representation, the following transformation could be applied in the case where P is significantly greater than N

$$P_j = \sum_{n=1}^{P} T_{jn}\, c_n \qquad j = 1, \ldots, N \qquad (56)$$

where

$$T_{jn} = \int_{x_{j-1}}^{x_j} \sigma_x(x)\ \phi_n(x)dx, \quad x_0 = 0,\ x_n = 1 \tag{57}$$

and

$$m_j = \int_{x_{j-1}}^{x_j} \sigma_x(x)\ dx \Big/ \int_0^1 \sigma_x(x)dx \quad j = 1, \ldots, N \tag{58}$$

define $\{x_j\}$ in terms of the mode-block partition $\{m_j\}$ so that the resulting transfer matrices would be independent of the choice of mode parameter x.

If a set of N measurements of input and output near-field patterns are made for an element of a system, then the N solutions to equation 52 for the input and output mode-power-distribution coefficients, or some transformation of them, can be used in equation 43 to find H, the transfer matrix for that element. Introducing the notation for an N by N matrix

$$V^{(\alpha)} = (\bar{v}_1|\bar{v}_2|\ldots|\bar{v}_N)^{(\alpha)} \tag{59}$$

where $\bar{v}_i$ are N by 1 column vectors and $\alpha = 0$, or 1 indicates input or output, respectively, the formal solution for H can be written

$$H = [A^{(1)}]^{-1}\ (\bar{b}_1|\ldots|\bar{b}_N)^{(1)}\ [(\bar{b}_1|\ldots|\bar{b}_N)^{(0)}]^{-1}\ A^{(0)} \tag{60}$$

which requires, not only that A have an inverse, but that the matrix made up of the vectors $\bar{b}_i$ obtained by equation 54 from the N input near-field patterns have an inverse, that is, that these N vectors be linearly independent. This requirement to have N independent input conditions places the practical upper limit on N and, consequently, the accuracy of reduced-dimension transfer matrix methods.

Similarly, N independent measurements of the response of a photodetector can be used to form a matrix equation whose formal

solution for the response vector is

$$\bar{r} = \bar{j} \; [(\bar{b}_1|\ldots|\bar{b}_n)^{(0)}]^{-1} \; A^{(0)} \tag{61}$$

where $\bar{j}$ is the row vector formed from the N photocurrent measurements.

While these equations represent solutions for H and $\bar{r}$, there are advantages obtained by not using them for numerical computation. Rather, a more robust technique such as a singular value decomposition of the input data matrix made up of the near-field pattern vectors should be used. Thus, rewriting the data matrix in terms of its singular-value decomposition

$$D^{(0)} = (\bar{c}_1|\ldots|\bar{c}_K)^{(0)} = USV^T \tag{62}$$

where now, K, the number of measurements, may be greater than N, the dimension of the desired reduced dimension transfer matrix. Not all K measured vectors need be independent. Now, from the pseudoreverse VS^+U^T of USV^T, a least-square fit to H can be found

$$H = (\bar{c}_1|\ldots|\bar{c}_K)^{(1)} \; VS^+U^T \tag{63}$$

without calculating explicitly $[D^{(0)} \; D^{(0)T}]^{-1}$. Furthermore, from consideration of the singular values contained in the diagonal matrix S a condition number for $D^{(0)}$ can be obtained that can be used to evaluate the magnitude of computational and random errors that might occur in H as a result of round off error in the computation and noise in the input and output data matrices. More importantly, the condition numbers can be used to ascertain the degree of independence of at least N of the K measured input data vectors.

Similar considerations militate towards the singular value decomposition of the input data matrix to obtain a least-square fit to the detector response vector from the output-current vector $\bar{j}$. In both cases, the input data matrices made up of the $\bar{c}$ vector columns, should be obtained by some robust technique, such as Cholesky decomposition of the symmetric A matrix applied to the primary data vector $\bar{b}$, rather than direct inversion of A.

MEASUREMENT CONSIDERATIONS

The general conditions under which the measurements should be made is that the apparatus remain optically and electronically stable for a given launch configuration during the time it takes to measure a pair of input and output near-field patterns for a component, the output current and input near-field pattern for a detector, or a sequence of output near-field patterns of a source. The near-field patterns, I(sa), are the radiant emittance on a fiber end face and they have the units of power per unit area. Typically, near-field patterns are determined from a relative measurement, M(u), of the radiant emittance of an enlarged image of the fiber end face, an absolute measurement of the total radiant flux from the fiber end, W, and a measurement of the fiber core area, πa^2. Thus,

$$I(as) = M(bs)/G \tag{64}$$

here the instrument gain, G, is defined to include the image magnification b/a, where b is the radius of the core image, as well as the electronic amplification. The gain is given by

$$G = \frac{\pi a^2 \int_0^b u\, M(u)\, du}{W \int_0^b u\, du} \quad . \tag{65}$$

Usually, the image coordinate, u, is scaled so as to make b approximately full scale.

The input radiometric quantity used to characterize optical detectors can be either flux (power) or irradiance (power per unit area), depending on the intended use of the detector. If the detector is to be irradiated with a spot of radiation that does not fill the detector, flux is generally chosen. If, on the other hand, the detector is to be overfilled with relatively uniform radiation, irradiance would be used. For fiber-optic systems, the detector can be expected to be underfilled, so that flux would be the expected choice. However, most measurements are related to the determination of transfer matrices of components, and if irradiance is chosen to be the quantity characterizing the system, it is not necessary to have values for either the first factor of G, equation 65, or the normalized frequency V, equation 24, to determine transfer matrices. This is because choosing irradiance rather than flux to characterize the power flow in the system is equivalent to using $V^2 p(x)/2\pi a^2$ rather than $V^2 p(x)/?$ to characterize the mode-power distribution. In any case, if the instrument gain were to be changed between the input and output near-field measurements of a pair, the gain ratio of the two measurements would have to be determined.

Of course, whatever the choice of characterizing radiometric quantity, in order to determine source or detector response vectors, the gain, G, is needed requiring measurements of both the core radius, a and the power, W. If an absolute determination of the mode-power distribution is desired, then, in addition, a value of the V parameter must be available.

The transfer matrices, as well as the source and detector response vectors, will be different by scalar factors for different choices of normalization units. For example, in the mode-block case, matrices determined with irradiance as the significant quantity must be multiplied by the ratio of the areas of the output to the input fiber cores in order to obtain the matrices corresponding to flux as the significant quantity. Consequently, for irradiance based transfer matrices, the upper limits for matrix-element and column-sum size become the ratio of input to output fiber core areas rather than one as it is for flux based transfer matrices (see TRANSFER MATRIX INTERPRETATION).

ALTERNATIVE VIEWPOINT

In addition to the mode-block and expansion-coefficient formalisms, other approaches to generating sets of consistent transfer matrices are possible. For example, the matrix A defined in equation 53 can be considered to be a transformation of the vector $\bar{c}$ into the vector $\bar{b}$ defined in equation 54. In such a representation, the measured transfer matrix becomes

$$H = (\bar{b}_1|\ldots|(\bar{b}_K)^{(1)} \quad [(\bar{b}_1|\ldots|\bar{b}_K)^{(0)}] \tag{66}$$

and the measured detector-response vector becomes

$$\bar{r} = \bar{J} \; [(\bar{b},|\ldots|\bar{b}_K)^{(0)}]^{+} \quad . \tag{67}$$

In this representation, neither the matrix A nor its inverse needs to be calculated.

Even greater simplification results if a transformation T on $\bar{b}$ can be found such that

$$q_i = \sum_{j=1}^{N} T_{ij} \; b_j \tag{68}$$

for which

$$\xi_i(s) = \sum_{j=1}^{N} T_{ij} \; \psi_j(s) \tag{69}$$

so that from equation 54

$$q_i = \int_0^1 sI(s) \; \xi_i(s) \; ds \tag{70}$$

where $\{\xi_i(s)\}$ is a set of orthogonal functions on the domain (0,1) with weighting function s. In this case, the set $\{q_i\}$ is the expansion coefficients of I(s) for the chosen set of orthogonal functions, for example, Jacobi polynomials, and are used in place of the $\{b_i\}$ to calculate transfer matrices. The transformation T and functions ψ_i are not explicitly required; however, their existence must be assumed. It has not yet been verified either theoretically or experimentally, but it seems plausible that they do exist from consideration of the differential form of equation 55 and the idea that sets of orthogonal functions can be found whose derivatives are also sets of orthogonal functions.

An advantage of this extension is that the index of refraction function, f(s), does not necessarily enter the calculation unless the mode-power distribution, p(x), is required, and the core radius, a, enters only relatively in the definition, $s = \rho/a$. Furthermore, if the $\{\xi_i(s)\}$ are chosen to be rectangular functions that are one for $0 = s_0 < s_1 \ldots < s_{i-1} < s \leq s_i < s_{i+1} \ldots < s_N = 1$ and zero otherwise, then the q_i are directly measurable as the power within an annulus in the near-field pattern. An appropriate choice for the partition $\{s_i\}$ might be in this case

$$\int_{s_{i-1}}^{s_i} s[1-f(s)]ds = \frac{1}{N}\int_0^1 s[1-f(s)]ds \tag{71}$$

reintroducing f(s) into the calculation of $\bar{q}$.

EQUIVALENCE OF REPRESENTATIONS

The various representations of the reduced-dimension transfer matrices can be related to one another through the full matrix of scattering coefficients, s, and the dimension-reducing transformations, T, corresponding to each of the reduced-dimension representations. Let

$$H = TsT^+ \tag{72}$$

be an M-dimensional representation of s and

$$\tilde{H} = \tilde{T}s\tilde{T}^+ \tag{73}$$

be an $\tilde{M}$-dimensional representation of s, then, in a best-possible sense,

$$H \approx T\tilde{T}^+\tilde{H}\tilde{T}T^+ \quad . \tag{74}$$

This relationship is only approximate because, while H and $\tilde{H}$, respectively, are defined by equations 72 and 73, it is generally true that

$$s \neq \hat{T}^{+}\hat{H}\hat{T} \tag{75}$$

because, in general, the information lost in conversion of s into $\hat{H}$ cannot be fully recovered. Consequently, equation 74 should be most useful if $M \leq \tilde{M}$.

For example, consider the transformation from a mode-block representation with $\tilde{M} = 3$ to one which has $M = 2$, where the partitions are related by the restriction $\tilde{m}_1 \leq m_1 \leq \tilde{m}_1 + \tilde{m}_2$. In this instance, equations 7 and 8 yield

$$T\hat{T}^{+} = \begin{bmatrix} 1 & \dfrac{m_1 - \tilde{m}_1}{\tilde{m}_2} & 0 \\ 0 & \dfrac{m_2 - \tilde{m}_3}{\tilde{m}_2} & 1 \end{bmatrix} \tag{76}$$

and

$$\hat{T}T^{+} = \begin{bmatrix} \dfrac{\tilde{m}_1}{m_1} & 0 \\ \dfrac{m_1 - \tilde{m}_1}{m_1} & \dfrac{m_2 - \tilde{m}_3}{m_2} \\ 0 & \dfrac{\tilde{m}_3}{m_2} \end{bmatrix} \tag{77}$$

so that, according to equation 74,

$$H_{11} \approx (\hat{H}_{11} + \frac{m_1-\tilde{m}_1}{\tilde{m}_2}\hat{H}_{21})\frac{\tilde{m}_1}{m_1} + (\hat{H}_{12} + \frac{m_1-\tilde{m}_1}{\tilde{m}_2}\hat{H}_{22})\frac{m_1-\tilde{m}_1}{m_1} \quad (78)$$

$$H_{21} \approx (\frac{m_2-\tilde{m}_3}{\tilde{m}_2}\hat{H}_{21} + \hat{H}_{31})\frac{\tilde{m}_1}{m_1} + (\frac{m_2-\tilde{m}_3}{\tilde{m}_2}\hat{H}_{22} + \hat{H}_{32})\frac{m_1-\tilde{m}_1}{m_1} \quad (79)$$

$$H_{12} \approx (\hat{H}_{12} + \frac{m_1-\tilde{m}_1}{\tilde{m}_2}\hat{H}_{22})\frac{m_2-\tilde{m}_3}{m_2} + (\hat{H}_{13} + \frac{m_1-\tilde{m}_1}{\tilde{m}_2}\hat{H}_{23})\frac{\tilde{m}_3}{m_2} \quad (80)$$

$$H_{22} \approx (\frac{m_2-\tilde{m}_3}{\tilde{m}_2}\hat{H}_{22} + \hat{H}_{32})\frac{m_2-\tilde{m}_3}{m_2} + (\frac{m_2-\tilde{m}_3}{\tilde{m}_2}\hat{H}_{23} + \hat{H}_{33})\frac{\tilde{m}_3}{m_2} \quad . \quad (81)$$

In contrast, the generalized mode-block reduction defined by equations 2, 12, and 13 provides in the case for which $M \leq \tilde{M}$ and the same set of discrete polynomials is used for both representations that $H_{ij} \approx \hat{H}_{ij}$; that is, H is a principal diagonal matrix of $\hat{H}$. This simple relationship is a result of the orthogonality of the basis functions for the two representations. Furthermore, by letting M be reduced to one, it follows that, in this case, H_{11} should be the scalar quantity best characterizing the transmission of power, or power per unit area as the case may be, through a component. In the mode-block case, the analogous scalar transmission for a component is given by the transformation

$$T\hat{T}^{+} = (1, 1, \ldots 1) \quad (82)$$

$$\underset{\sim}{T}\underset{\sim}{T}^{+} = (\frac{1}{\underset{\sim}{M}}, \frac{1}{\underset{\sim}{M}}, \ldots \frac{1}{\underset{\sim}{M}})^{T} \tag{83}$$

of the $\underset{\sim}{M}$ dimensional matrix $\underset{\sim}{H}$ to the one dimensional matrix H_{11}. This results in

$$H_{11} = \frac{1}{\underset{\sim}{M}} \sum_{i,j=1}^{\underset{\sim}{M}} \underset{\sim}{H}_{ij} \quad . \tag{84}$$

In general, the matrix T that transforms s into H will not be available, so an alternative approximate transformation between representations is desirable. Suppose that the power-flow vectors for the two representations can be related by a transformation Q such that $\bar{c} = Q\tilde{\bar{c}}$. If $\bar{c}' = H\bar{c}$ and $\tilde{\bar{c}}' = \underset{\sim}{H}\tilde{\bar{c}}$, then

$$Q^{+}Q\ \tilde{\bar{c}}' \approx Q^{+}Q\ \underset{\sim}{H}\ Q^{+}\ Q\bar{c} \tag{85}$$

or

$$\bar{c}' \approx Q\underset{\sim}{H}\ Q^{+}\ \bar{c} \tag{86}$$

where Q^{+} is the generalized inverse of Q, defined so that $\tilde{\bar{c}} \approx Q^{+}\bar{c}$ so that $Q^{+}Q \approx I$. Hence,

$$H \approx Q\underset{\sim}{H}\ Q^{+} \tag{87}$$

that is, Q and Q^{+} replace $T\underset{\sim}{T}^{+}$ and $\underset{\sim}{T}T^{+}$, respectively. Now if the mode-power distribution can be approximated either by

$$p(x) \approx \sum_{i=1}^{M} c_i\ \phi_i(x) \tag{88}$$

or

$$p(x) \approx \sum_{i=1}^{\tilde{M}} \tilde{c}_i \, \tilde{\phi}_i(x) \tag{89}$$

where $\{\phi_i\}$ and $\{\tilde{\phi}_i\}$ are sets of orthogonal functions such that

$$\int_0^1 w(x) \, \phi_i \, \phi_j(x) dx = \delta_{ij} \tag{90}$$

and

$$\int_0^1 \tilde{w}(x) \, \tilde{\phi}_i(x) \, \tilde{\phi}_j(x) dx = \delta_{ij} \quad . \tag{91}$$

It then follows that

$$c_i \int_0^1 w(x) \, \phi_i^2(x) dx \approx \sum_{j=1}^{\tilde{M}} \left[\int_0^1 w(x) \phi_i(x) \tilde{\phi}_j(x) dx \right] \tilde{c}_j \tag{92}$$

so that

$$Q_{ij} \approx \frac{\int_0^1 w(x) \phi_i(x) \tilde{\phi}_j(x) dx}{\int_0^1 w(x) \phi_i{}^2(x) dx} \quad . \tag{93}$$

Similarly,

$$Q_{ij}^{+} \approx \frac{\int_0^1 \tilde{w}(x) \tilde{\phi}_i(x) \phi_j(x) dx}{\int_0^1 \tilde{w}(x) \, \tilde{\phi}_i{}^2(x) dx} \quad . \tag{94}$$

Transformations within sets of basis functions, that is, where $\{\tilde{\phi}_i\} = \{\phi_i\}$, yield immediately the simple result that $\hat{H}_{ij} \approx H_{ij}$, $i,j = 1, \ldots, M$, where $M \leq \tilde{M}$, just as previously obtained.

In the case of a mode-block representation, the $\{\phi_i\}$ are the rectangular functions and $w(x)$ is proportional to the mode

density, $\sigma(x)$. The case of a transformation between two mode-block representations can be simplified if the representations have been defined in terms of a fractional number of modes per block, as in the use of equation 58, so that the mode density $\sigma(x)$ can be taken to be uniform even though it may not have been in the original experimental determination, as in the use of equation 23. In this situation, the Q_{ij} represent the overlap of the $\{\tilde{m}_i\}$ blocks on the $\{m_i\}$ blocks and the reverse for Q^+_{ij}, and the use of diagrams such as those shown figures 1 and 2 can aid in evaluating this overlap. For example, consider a transformation from $M = 2$ to $\tilde{M} = 3$, where, for simplicity, the mode-partitions satisfy the restriction $m_1 \geq \tilde{m}_1 + \tilde{m}_2$. Aided by figure 1, we obtain from equation 93

$$Q = \begin{bmatrix} 1 & 1 & \dfrac{\tilde{m}_3 - m_2}{\tilde{m}_3} \\ 0 & 0 & \dfrac{m_2}{\tilde{m}_3} \end{bmatrix} \tag{95}$$

and aided by figure 2 we obtain from equation 94

$$Q^+ = \begin{bmatrix} \dfrac{\tilde{m}_1}{m_1} & 0 \\ \dfrac{\tilde{m}_2}{m_1} & 0 \\ \dfrac{\tilde{m}_3 - m_2}{m_1} & 1 \end{bmatrix} . \tag{96}$$

Equation 87 could now be applied to obtain the relation between the matrix elements of the two transfer matrices. Notice that

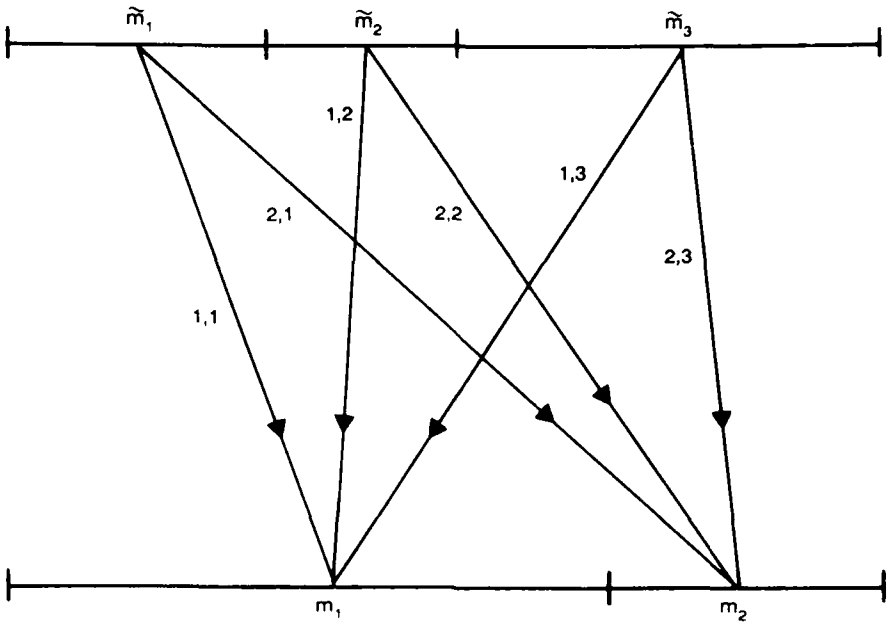

Figure 1. Aid for obtaining the matrix elements in equation 95.

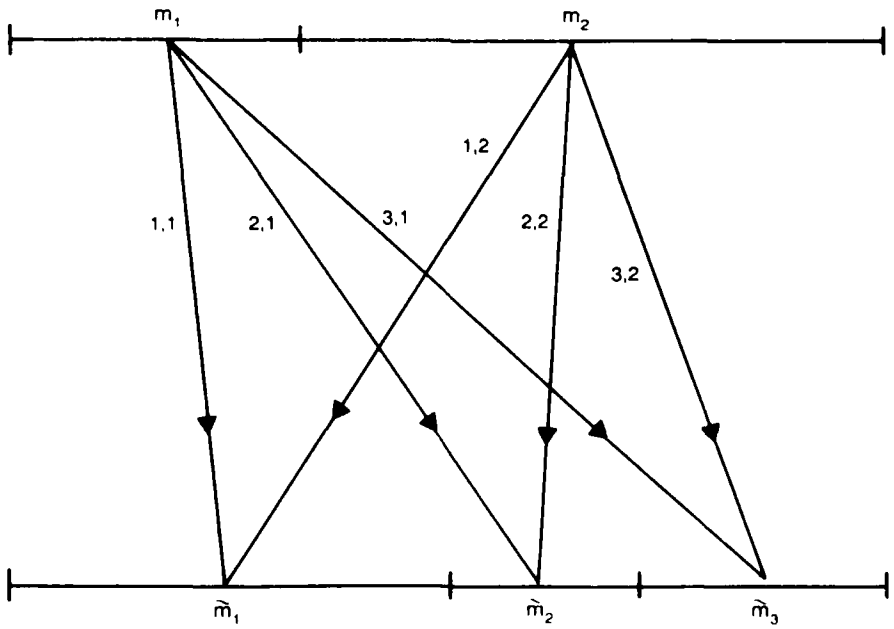

Figure 2. Aid for obtaining the matrix elements in equation 96.

here as well as in the earlier example, the column sums of the transformation matrices add to one.

Although we have shown that all representations are equivalent in the sense that one can be obtained approximately from another, it must be kept in mind that each transformation causes some of the information that was contained in the original measurements of the near-field patterns to be lost. Consequently, whenever it is possible, original data should be used or augmented to make new calculations rather than attempting to transform previously determined matrices.

TRANSFER MATRIX INTERPRETATION

Except in the mode-block approach, the basis functions for the expansion of the mode-power distribution are oscillating functions; consequently, there is no simple general physical interpretation of the vector components or of the transfer-matrix elements, which can be either positive or negative and of unpredictable magnitude. Discussion of the mode-block interpretation is postponed until following the mention of two special cases in which the lowest order component of a state vector, $\bar{c}$, can be related to the total optical power flow.

The first case is obtained by choosing a representation for which $\bar{c}$ is proportional to $\bar{q}$, defined by equations 68 to 70, and noting that ξ_1, the lowest order function, is a constant. The second case arises if the weighting function, $w(x)$, of the $\{\phi_n(x)\}$

is chosen to be the mode density, $\sigma_x(x)$, defined by equations 19 to 22. In these two cases, respectively, equations 19 and 29 for the power flow yield

$$q_1 = \frac{W}{2\pi a^2} \xi_1 \tag{97}$$

where ξ_1 is a constant, and, noting that $\phi_1 = 1/\sqrt{N}$,

$$c_1 = \frac{W}{\sqrt{N}} \tag{98}$$

where N is the number of propagating modes.

In contrast, for the mode-block approach, the physical interpretation of the vector components and transfer-matrix elements provides information about the range of possible transmission coefficients for a component. By definition, the components of the mode distribution vector $\bar{u}$ are the amount of power flowing in a mode, so $u_i \geq 0$ for i = 1, ..., N. Since the elements of the scattering matrix, s, represent the fraction of power scattered from one mode into another, $0 \leq s_{ij} \leq 1$ for i,j = 1, given by

$$W' = \sum_{i=1}^{N} u'_i \tag{99}$$

can be written in terms of the input mode vector

$$W' = \sum_{i=1}^{N} T_i \, u_i \tag{100}$$

where the column sum

$$T_i = \sum_{j=1}^{N} s_{ji} \tag{101}$$

thus, $T_{min}\ W \le W' \le T_{max}\ W$, where W is the input power and T_{min} and T_{max} are the smallest and largest column sums of s. Consequently, $0 \le T_i \le 1$, i = 1, ..., N. It follows from the general definition of a reduce-dimension transfer matrix, equation 4, that the column sums

$$S_j = \sum_{i=1}^{M} H_{ij} \quad , \ j = 1, \ldots, M \tag{102}$$

can be rewritten as

$$\sum_{k,l=1}^{N} \left(\sum_{i=1}^{M} T_{ik}\right) s_{kl}^{+} T_{lj} = \sum_{l=1}^{N} T_l \, T_{lj}^{+} \quad . \tag{103}$$

Thus,

$$T_{min} \le S_j \le T_{max} \tag{104}$$

where the fact that the column sums of the relevant mode-block transformations T and T^+ are all equal to one has been used. Since $0 \le H_{ij}$, i, j = 1, ..., M, it follows from equation 104 that $0 \le H_{ij}, S_j \le 1$, which is consistent with the interpretation of the elements of the reduced-dimension mode-block transfer matrix as being a best approximation to the fraction of input power in a mode-block scattered into another mode-block on output.

Equation 100 can be rewritten as

$$W' = T(\bar{u})W \tag{105}$$

where $T(\bar{u})$ is the power transmission coefficient of the component for an input mode distribution $\bar{u}$. Thus,

$$T(\bar{u}) = \frac{\sum_{i=1}^{N} T_i \, u_i}{\sum_{i=1}^{N} u_i} \quad . \tag{106}$$

Similarly an estimate of this power transmission coefficient is

$$T(\bar{c}) = \frac{\sum_{i=1}^{M} S_i \, c_i}{\sum_{i=1}^{M} c_i} \tag{107}$$

where by equation 2 $\bar{c} = T\bar{u}$. Clearly, $T_{min} \leq T(\bar{u})$, $T(\bar{c}) \leq T_{max}$ and $S_{min} \leq T(\bar{c}) \leq S_{max}$, where S_{min} and S_{max} are, respectively, the smallest and largest column sums of H.

That the range of predicted transmission coefficients can be seen immediately from the column sums S_{min} and S_{max} of the reduced-dimension transfer matrix in mode-block form is useful, but this does not provide a reliable estimation of the range of observable transmission coefficients determined by T_{min} and T_{max} unless the partition of the mode distribution has been made into small enough blocks so that it is unlikely that any mode distribution can develop with power predominantly in one block, assuring that the average implied in equation 106 is carried out over at least a block. This, of course, makes the measurement of a mode transfer matrix difficult at best.

If the column sums $T_{min} = T_{max}$, then also the column sum $S_j = S$, $j = 1, \ldots, M$, and $W' = S\,W$ and such an element would be an ideal attenuator. If two ideal attenuators are concatenated, the resulting composite system will also be an ideal attenuator with $S^{12} = S^1 S^2$. It would appear that ideal attenuators can be fully characterized by a scalar transmission coefficient and that systems made up of such ideal components would not exhibit the

concatenation effect; however, this would be true if only power flow were of interest. If the signal response is considered as in equation 48, it is evident that

$$r_{min}\, S_{min}\, W \leq j \leq r_{max}\, S_{max}\, W \qquad (108)$$

where r_{max} and r_{min} are, respectively, the largest and smallest photodetector-response-vector components. Therefore, unless the photodetector is characterized by a uniform vector with $r_{min} = r_{max}$, the observed photocurrent will show the concatenation effect even though it may be true that $S_{min} = S_{max}$. In general, only systems made up of components whose characterizing transfer matrices commute will not be subject to the concatenation effect.

The benefits of the physical interpretation of components represented by the mode-block formalism can, in principle, be extended to other representations through a transformation as in equations 87, 93, and 94, the column sums then being evaluated in the resulting mode-block representation.

EQUILIBRIUM MODE DISTRIBUTION

The eigenvectors, $\bar{v}_n$, and eigenvalues, λ_n, of scattering matrices play an important role in their physical interpretation. The eigenvectors of a scattering matrix of a component represent the mode-power distributions that when launched into a component appear unchanged at the output except for an attenuation factor λ, the associated eigenvalue. Consequently, if steady state or equilibrium mode distributions exist in sequences of repeated components, they are given by the eigenvector of the scattering

matrix associated with the largest eigenvalue, that is, greatest transmission provided it represents a physically realizable distribution.

The eigenvectors and eigenvalues of a reduced-dimension transfer matrix should have a similar interpretation to those of the full scattering matrix. However, it is not clear that enough information is retained in the reduced dimension to make the predicted equilibrium distributions useful. That is, after a number of passes, say k, through a component does the occurrence of the product $T^{+}T$ k-1 times, see equation 16, diminish the suitability of the reduced-dimension transfer matrix H^{k} faster than the output approaches the equilibrium distribution? The difficulty here is analogous to those that arise in considerations of the concept of expressing a transfer matrix in decibels, which requires that the matrix be written as

$$H = \exp(a)^{A} = \sum_{n=1}^{\infty} \frac{1}{n!} A^{n} \qquad (109)$$

where 10 log A is the matrix representation of H in decibels (references 12, 25, and 29). The question being, does the error in A^{n} due to uncertainty in A increase more rapidly with n than the series converges? Caution should be exercised when using eigenvectors of reduced-dimension transfer matrices to predict equilibrium mode distributions.

COMPUTER PROGRAMS

Three computer programs using the integral form of the mode-power/near-field relationship for converting near-field-pattern data into reduced-dimension transfer matrices, detector response vectors, or source vectors have been written in FORTRAN and are available on IBM compatible MS-DOS format diskette from the author. The first of these programs uses the mode-block reduction. The other two reductions are based on orthogonal polynomial expansions of the mode-power distribution. One of these carries out the expansion to a large number of terms, say 10, and then truncates the expansion at the number of terms equal to the dimension of the reduced-dimension transfer matrix, while the other carries out the expansion only to the desired dimension of the reduced matrix from the start. These may differ somewhat in the final result primarily because the weight function used in the least-square fit is not necessarily the same as that characterizing the orthogonal polynomials, but also because the mode-power distribution appears in an integral in the least-square-fit error function.

In all three programs, alpha index of refraction profiles and beta mode densities were assumed (see equations 32 and 33), and the choice between Chebyshev and Jacobi orthogonal polynomials with weight functions $1/\sqrt{x(1-x)}$ and x, respectively, over the domain (0,1) is offered. The mode-block program uses a mode-fraction partition so, except for computation error, the

transfer matrices generated by it should be independent of the choice of beta (beta must not be zero) as well as the selected set of polynomials. The other two programs should produce results that depend on these choices. In all three cases, the value used for alpha should correspond to the actual index of refraction profile of the fiber. For simplicity the programs assume that alpha is the same for both the input and output fibers. However, the core diameter as well as the normalized frequency may be different for the input and output fibers. Also, source and detector vectors are referred to power-per-unit area. All three programs use singular-value decomposition to obtain the pseudoinverse of the measurement matrix. Consequently, as many measurement sets as are available can be incorporated into a least-square determination of a transfer matrix, and the condition number of the measurement matrix is reported to permit selection of the largest acceptable dimension for a transfer matrix.

Also available on diskette from the author are two programs to determine a suitable value for alpha from either near-field pattern data, presuming a uniform mode distribution, or index of refraction profile data. In the first case, the data are fitted by a function of the form

$$c_1 \frac{(1 - \rho/a)^{\alpha}}{\sqrt{1 - K\,(\rho/a)^2}} + c_0 \qquad (110)$$

where non-zero K accounts for leaky modes (reference 1), and in the second case, by a function of the form

$$c_2\,[1 - (\rho/a)^{\alpha}] + c_1(\rho/a)^{\alpha} + c_0 \quad . \qquad (111)$$

The coefficients c_0, c_1, and c_2 as well as α and K are determined from data given as a function of ρ/a.

BANDWIDTH CHARACTERIZATION

The transfer-matrix formalism presented in this report can be extended to include bandwidth as well as loss characterization. Even though bandwidth chracterization has not yet been fully formulated and is outside the scope of this report, a brief description of a possible approach for doing so would seem in order (reference 11).

The basic assumption is that equation 1 can be extended to include a time dependence in the mode-power distribution simply by changing the form to

$$u_i'(t) = \sum_{j=1}^{N} \int_{-\infty}^{\infty} s_{ij}(t-\tau) u_j(\tau) d\tau \qquad (112)$$

where now $0 \leq s_{ij}(t) \leq 1$ is to be interpreted as an impulse response for scattering of power from the jth input mode into the ith output mode.

For a concatenated system consisting of two elements characterized by $s^{(1)}$ and $s^{(2)}$

$$u_i'(t) = \sum_{r,j=1}^{\infty} \int_{-\infty}^{\infty} \int_{-\infty}^{\infty} s_{ir}^{(2)}(t-\tau_2)\, s_{rj}^{(1)}(\tau_2 - \tau_1) u_j(\tau_1) d\tau_1 d\tau_2 \quad . (113)$$

By taking Fourier transforms of both sides equation 113, the sums of convolution integrals in the time domain may be replaced by matrix products in the frequency domain; thus,

$$\bar{u}'(\omega) = s^{(2)}(\omega)\ s^{(1)}(\omega)\ \bar{u}(\omega) \tag{114}$$

where the Fourier transform relationship is indicated by replacing the time argument, t, by the frequency argument, ω. The time dependent quantities $\bar{u}(t)$ and $s(t)$ are real; however, in general, the frequency dependent Fourier transforms $\bar{u}(\omega)$ and $s(\omega)$ are complex except for $\omega = 0$, where they are real and correspond to the case of simple loss characterization treated in the bulk of this report.

Just as in the case of loss characterization, a frequency independent transformation T can be introduced to define a reduced-dimension scattering matrix $M(\omega)$, where

$$M(\omega) = T\ s(\omega)\ T^{+} \quad . \tag{115}$$

Also, in order to provide a measurable approximation $H(\omega)$ to $M(\omega)$, a frequency dependent continuous mode power distribution $p_x(x,\omega)$, which can be related to the Fourier transform of the time dependent observed near-field pattern I(s,t), can be introduced. Thus,

$$I(s,\omega) = \frac{V^2}{2\pi a^2} \int_{f(s)}^{1} p_x(x,\omega)dx \tag{116}$$

furthermore,

$$p_x(x,\omega) = \sum_{i=1}^{p} c_i(\omega)\phi_i(x) \tag{117}$$

where the complex coefficients $c_i(\omega)$ become the reduced dimension representation of $u(\omega)$.

The determination of the complex vector $\bar{c}(\omega)$ can be carried out by least-square fitting as before from equation 51, where the matrix A is real and identical to the loss characterization case and the complex vector $\bar{b}(\omega)$ must be found from measurements of the Fourier transform of I(s,t); thus

$$b_i(\omega) = \frac{V^2}{2\pi a^2} \int_0^1 s\, I(s,\omega) \int_{f(s)}^1 \phi_i(x)dx\, ds \quad . \qquad (118)$$

We see that the near-field pattern measurements now have the additional complication of requiring phase as well as amplitude to be determined at each point in the pattern over the expected modulation bandwidth of the system.

Once the vectorization process, that is, the determination of $\bar{b}(\omega)$ from $I(s,\omega)$, is complete, then input and output data matrices $(\bar{c}_1(\omega)|\ldots|\bar{c}_p(\omega))$ and $(\bar{c}_1'(\omega)|\ldots|\bar{c}_p'(\omega))$, respectively, can be formed and $H(\omega)$ determined according to equation 63. This determination is complicated by the complex vectors, $\bar{c}(\omega)$, involved, but the essential question is: out of the p measured input vectors $\bar{c}_i(\omega)$, are there at least N, where $N \leq P$ is the dimension of H, independent complex vectors? The answer is yes if an ideal chopped modulation is assumed, that is, it is sufficient that the input near-field patterns can be written in the separated form $I(s,\omega) = I(s)F(\omega)$, where $F(\omega)$ is a complex function of unit amplitude. The M vectors $\bar{b}(\omega)$ are simply real vectors multiplied by a complex scalar, and the resultant $\bar{c}_i(\omega)$ will be independent to the same degree as could be achieved in simple loss characterization.

Here only component transfer matrices and source vectors have been mentioned, but the detector response vector $\bar{r}(\omega)$ could be similarly determined and would, in general, be complex as would the resulting signal current $j(\omega)$.

Once all of the components of a system have been characterized, the total system loss and bandwidth, based on consideration of $|j(\omega)|^2$, can be predicted from the product of component matrices and the detector-response and source vectors. It should be noted that even matrices that have only real, frequency independent elements, as would be expected of small sized passive components, must be included in the product as they would influence not only the loss but the bandwidth determined in this approach as well.

If a mode-block basis is used, an upper limit on frequency response of a system can be expressed in terms of the column sums of the absolute values of the constituent component matrices. Consider, for example, a system characterized by

$$j(\omega) = \bar{r}\ (\omega) \bullet H^{(2)}(\omega)H^{(1)}(\omega)\bar{c}(\omega) \quad . \tag{119}$$

From the submultiplicative property of the maximum column sum matrix norm (reference A-2, section 5.6), it follows that

$$|j(\omega)| \leq ||\bar{r}(\omega)||_1||H^{(2)}(\omega)||_1||H^{(1)}(\omega)||_1||\bar{c}(\omega)||_1 \tag{120}$$

where, for an M by M matrix A

$$||A||_1 = \max_{1\leq j\leq M} \sum_{i=1}^{n} |A_{ij}| \quad . \tag{121}$$

Evidently the contribution of each component to this upper limit can be obtained independently; however, because this upper limit

can be well beyond actual performance, caution must be exercised in using such limits.

SUMMARY

We have shown that a reduced-dimension transfer matrix can be defined in terms of a rectangular matrix transformation from the full-dimension mode space to a reduced-dimension space and its psuedoinverse. Furthermore, we have shown that the reduced-dimension space need not be the conventional mode-block partition. Although the reduced-dimension transfer matrices are in some sense the best possible approximation to the full transfer matrix, as a consequence of this definition, the product of reduced dimension transfer matrices inevitably deviates from the reduced dimension representation of the product of full dimension matrices.

We have presented a least-square-fit method that, to a large extent, circumvents errors resulting from having to compute the derivative of noisy data, as is required in the conventional method, and permits the natural inclusion of additional data sets beyond the minimum number of the dimension of the reduced representation. As a consequence of using singular-value decomposition in this method, the condition number of the data matrix is obtained and provides a measure of the independence of the launch conditions, which is essential to the success of measurements of transfer matrices.

We have shown that all reduced-dimension representations are equivalent in the sense that one can be obtained from another without knowledge of the full representation, although to do so results in some unavoidable loss in information. Consequently, valid reduced-dimension representations should be attainable directly from vectorization of the near-field patterns without first developing the mode distribution.

In addition to the consideration of loss characterization by transfer matrix, we have briefly touched upon the extension of the transfer matrix approach to bandwidth characterization. This extension needs both experimental and theoretical development to be useful for applications.

Computer programs written in FORTRAN-77 for the computation of various representations of reduced dimension transfer matrices from near-field patterns are available from the author.

REFERENCES

1. Gekler, S. 1987. *Optical Fiber Transmissions Systems*, ch. 6, Artech House, Inc., Norwood, MA.

2. Cancellieri, G., and U. Ravaioli. 1984. *Optical Fibers and Devices: Theory and Experiment*, Artech House, Inc., Dedham, MA.

3. Okoshi, T. 1982. *Optical Fibers*, ch. 5, Academic Press, NY.

4. Gowar, J. 1984. *Optical Communication Systems*, ch. 6, Prentice Hall International, Inc., London.

5. Holmes, G. T. 1981. "Estimation of Concatenated System Response Based on Measured Transfer Functions for Low and High Order Modes," 7th European Conference on Optical Communications, Copenhagen, September 8-11.

6. Agarwal, A. K., G. Evers, and U. Unrau. 1983. "Concatenation Effect Calculation for Fiber Optic Components From Measured 3 x 3 Mode Transition Matrices," 9th European Conference on Optical Communication, pp. 255-258, H. Melchior and A. Sollberger, Eds., Elsevier Science Publishers, B.V. (North Holland).

7. Maisonneuve, J. M., and R. L. Gallawa. 1984 and 1987. "The Use of Power Transfer Matrices in Predicting System Loss: Theory and Experiment," *Proceedings of SPIE, vol. 500, Fiber Optics: Short-Haul and Long-Haul Measurements and Applications II*, Robert L. Gallawa, Ed., pp. 88-93 and *Fiber and Integrated Optics*, vol. 6, number 1, pp. 11-26.

8. Evers, G., A. Kober, and U. Unrau. 1984. "Measurement of Mode Transition Matrices of Quasi-Step Index Optical Fiber Components," *Proceedings of SPIE, Vol. 500, Fiber Optics: Short-Haul and Long-Haul Measurements and Applications II*, Robert L. Gallawa, Ed., pp. 94-99.

9. Evers, G. 1985. "Mode Transition Matrices for Fiber Optic Connectors," *Electronic Letters*, 21, #9, pp. 401-402.

10. Maisonneuve, J. M., P. Churoux, and R. L. Gallawa. 1985. "Use of Mode Transfer Matrices in L. A. N. Loss Evaluation," *Proceedings of SPIE, vol. 559, Fiber Optics: Short-Haul and Long-Haul Measurements and Applications II*, pp. 182-185.

11. Evers, G. 1988. "Calculation and Measurement of Mode Transition Matrices for Differential Mode Attenuation and Differential Mode Delay Characterization of Optical Fiber," *Optical Engineering*, 27, #2, pp. 179-186.

12. Vayshenker, I. P., D. R. Hjelme, and A. R. Michelson. 1986. "Multimode Fiber Systems Characterization," *Technical Digest Symposium on Optical Fiber Measurements*, G. W. Day and D. L. Franzen, Eds., pp. 85-88.

13. Evers, G., and U. Unrau. 1986. "Assessment of Modal Effects in Local Area Networks," *Electronic Letters*, vol. 22, no. 16, pp. 859-861.

14. Gloge, D. 1971. "Weakly Guided Fibers," *Applied Optics*, vol. 10, no. 10, pp. 2252-2258.

15. Gloge, D. 1972. "Optical Power Flow in Multimode Fibers," *The Bell System Technical Journal*, vol. 51, no. 8, pp. 1767-1783.

16. Michelson, A. R., and M. Eriksrud. 1982. "Mode-Continuum Approximation in Optical Fibers," *Optics Letters*, vol. 7, no. 11, pp. 572-574.

17. Hawakami, S., and H. Lanji. 1983. "Evolution of Power Distribution in Graded-Index Fiber," *Electronics Letters*, vol. 19, no. 3, pp. 100-102.

18. Daido, Y., E. Miyauchi, T. Iwama, and T. Otsuka. 1979. "Determination of Modal Power Distribution in Graded-Index Optical Waveguides from Near-Field Patterns and Its Application to Differential Mode Attenuation Measurement," *Applied Optics*, vol. 18, no. 13, pp. 2207-2213.

19. Piazzola, S., and G. DeMarchis. 1979. "Analytical Relations Between Modal Power Distributions and Near-Field Intensity in Graded-Index Fibers," *Electronics Letters*, vol. 15, no. 22, pp. 721-722.

20. DeVita, P., and U. Rossi. 1980. "Realistic Evaluation of Coupling Loss Between Different Optical Fibers," *J. Opt. Commun.*, vol. 1, pp. 26-32.

21. Leminger, O. G., and G. K. Grau. 1980. "Near-Field Intensity Distribution in Multimode Graded-Index Fibers," *Electronics Letters*, vol. 16, no. 17, pp. 678-679.

22. Grau, G. K., and O. G. Leminger. 1981. "Relations Between Near-Field and Far-Field Intensities, Radiance, and Modal Power Distribution of Multimode Graded-Index Fibers," *Applied Optics*, vol. 20, no. 3, pp. 457-459.

23. Calavara, M., P. DeVita, and U. Rossi. 1981. "Reliability of a New Method for Measurements of Modal Power Distribution in Optical Fibers with Application to Mode Scrambler Testing," *Electronics Letters*, vol. 17, no. 15, pp. 543-545.

24. Rittich, D. 1985. "Practicability of Determining the Modal Power Distribution by Measured Near and Far Fields," *Journal of Lightwave Technology*, vol. LT-3, no. 3, pp. 652-661.

25. Michelson, A. R., and M. Eriksrud. 1983. "Mode-Dependent Attenuation in Optical Fibers," *J. Opt. Soc. Am.*, vol. 73, no. 10, pp. 1282-1290.

26. Yang, S., D. R. Hjelme, I. P. Januar, I. P. Vayshenker, and A. R. Michelson. 1988. "Single Launch Technique for Determination of Mode Transfer Matrices," *Technical Digest Symposium on Optical Fiber Measurements, NBS Special Publication 748*, pp. 103-105.

27. Yang, S., I. P. Vayshenker, D. R. Hjelme, and A. A. Mickelson. 1989. "Transfer Function Analysis of Measured Transfer Matrices," *Applied Optics*, vol. 28, no. 15, pp. 3148-3157.

28. Scheid, F. *Theorems and Problems of Numerical Analysis*, Second Edition, Schaum's Outline Series, McGraw Hill Book Company, ch. 23.

29. Moler, C. R., and C. F. VanLoan. 1978. "Nineteen Dubius Ways to Compute the Exponential of a Matrix," *SIAM Review*, vol. 20, pp. 801-836.

APPENDIX A. MATHEMATICAL BACKGROUND

GENERALIZED INVERSE (references A1 and A2)

The least-square problem to find an x to minimize $||\bar{A}x-\bar{b}||_2$, where A is an m by n matrix, $\bar{x}$ and $\bar{b}$ are n and m component vectors, respectively, and $||\bullet||_2$ is the Euclidean vector norm, has the unique solution

$$\bar{x}_{LS} = (A^H A)^{-1} A^H \bar{b} \tag{A1}$$

where A^H is the Hermitian transpose of A, if the rank of A is n, that is, if the columns of A are linearly independent. Otherwise, the vector $\bar{x}_{LS}$ such that $||\bar{x}||_2$ is minimized among all those $\bar{x}$ that produce the minimal $||A\bar{x}-\bar{b}||_2$ may be obtained from

$$\bar{x}_{LS} = A^+ \bar{b} \tag{A2}$$

where A^+, an n by m matrix, is typically defined to be the unique matrix that satisfied the Moore-Penrose conditions

$$A\ A^+\ A = A \tag{A3}$$

$$A^+\ A\ A^+ = A^+ \tag{A4}$$

$$(A\ A^+)^H = A\ A^+ \tag{A5}$$

$$(A^+\ A)^H = A^+\ A \tag{A6}$$

and is known as the Moore-Penrose generalized or pseudoinverse of A. A property of particular importance here is that $X = A^+$ is the unique matrix that minimizes the Frobinius matrix norm $||AX-I_m||_F$, where I_m is the m by m unit matrix.

SINGULAR-VALUE DECOMPOSITION (references A3 and A4)

Any m by n matrix A of rank r can be decomposed into the factored form

$$A = U \sum V^H \tag{A7}$$

where U and V are m by m and n by n unitary matrices respectively and $\sum$ is an m by n diagonal matrix with elements σ_r such that

$$\sigma_1 \geq \sigma_2 \sigma \geq \ldots \geq \sigma_{r+1} = \ldots = \sigma_q = 0 \tag{A8}$$

in which q is the lesser of m and n. The σ_r are uniquely determined by A, being the square root of the eigenvalues of AA^H, and the non-zero σ_r are known as the singular values of A. In terms of the singular-value decomposition, the generalized inverse of A can be written

$$A^+ = V \sum^+ U^H \tag{A9}$$

where $\sum^+$ is a n by m diagonal matrix with elements d_i such that

$$d_i = \frac{1}{\sigma_i} \quad , \quad i = 1, \ldots, r \quad . \tag{A10}$$

Thus, the singular-value decomposition provides a means to determine A^+. Stable algorithms for carrying out least-square solutions by singular-value decomposition without explicit determination of the eigenvalues of AA^H are available and only require about three times the computational effort as other least-square approaches (reference A5).

LEAST-SQUARE PERTURBATION (references A1 and A5)

Suppose we have solutions $\bar{x}_{LS}$ and $\bar{y}_{LS}$ to the least-square problems $||A\bar{x}-\bar{b}||_2$ minimized and $||(A+\delta A)\bar{y}-(\bar{b}+\delta\bar{b})||_2$ minimized, where both A and its perturbation $A+\delta A$ are m by n matrices with

$m \geq n$ and of full rank n and $\bar{b}$ and its perturbation $\delta\bar{b}$ are m dimensional vectors with $\bar{b} \neq 0$. The difference in these two solutions satisfies to first order in ε the relationship

$$\frac{||\bar{y}_{LS}-\bar{x}_{LS}||_2}{||\bar{x}_{LS}||_2} \leq \varepsilon K (2 + K \sin \Theta)/\cos \Theta \qquad \text{(A11)}$$

where we assume that

$$\varepsilon = \max \left[\frac{||\delta A||_2}{||A||_2}, \frac{||\delta\bar{b}||_2}{||\bar{b}||_2} \right] < \frac{1}{K} \qquad \text{(A12)}$$

and that

$$\sin \Theta = \frac{||A\bar{x}_{LS}-\bar{b}||_2}{||\bar{b}||_2} \neq 1 \qquad \text{(A13)}$$

with K, the condition number of A, equal to $||A||_2 \, ||A^+||_2 = \sigma_1/\sigma_n$ the ratio of the maximum to minimum singular values of A. Equation A11 gives an upper bound on the difference between the solutions of a least-square problem and its perturbation and as such may be much larger than the actual difference. However, it would be wise to be cautious when large values of condition number occur because, in contrast to the linear equation case, where m=n, differences can be magnified by the square of K for poorly fitting solutions. Furthermore, the magnification could be even greater than indicated by equation A11 for situations where A is not of full rank.

REFERENCES

A1. Golub, G. H., and C. F. VanLoan. 1983. *Matrix Computations*, sec 6.1, The Johns Hopkins University Press.

A2. Horn, R. A., and C. R. Johnson. 1985. *Matrix Analysis*, p. 421, Cambridge University Press.

A3. Stewart, G. W. 1973. *Introduction to Matrix Computations*, sec. 6.6, Academic Press.

A4. Reid, J. G. 1983. *Linear System Fundamentals*, appendix E., McGraw-Hill Book Company.

A5. Stewart, G. W. 1977. "On the Perturbation of Pseudo-Inverses, Projections and Linear Least Squares Problems," *SIAM Review*, vol. 19, no. 4, pp. 634-662.

REPORT DOCUMENTATION PAGE

Form Approved
OMB No. 0704-0188

1. AGENCY USE ONLY *(Leave blank)*	2. REPORT DATE	3. REPORT TYPE AND DATES COVERED
	December 1989	Final

4. TITLE AND SUBTITLE
TRANSFER MATRICES FOR MULTIMODE OPTICAL FIBER SYSTEMS

5. FUNDING NUMBERS
PE: 602233N
RM: 33R60, EE97
DN: 305061

6. AUTHOR(S)
C. J. Gabriel

7. PERFORMING ORGANIZATION NAME(S) AND ADDRESS(ES)
Naval Ocean Systems Center
San Diego, CA 92152-5000

8. PERFORMING ORGANIZATION REPORT NUMBER
NOSC TD 1717

9. SPONSORING/MONITORING AGENCY NAME(S) AND ADDRESS(ES)
David Taylor Research Center
Bethesda, MD 20084

10. SPONSORING/MONITORING AGENCY REPORT NUMBER

11. SUPPLEMENTARY NOTES

12a. DISTRIBUTION/AVAILABILITY STATEMENT
Approved for public release; distribution is unlimited.

12b. DISTRIBUTION CODE

13. ABSTRACT *(Maximum 200 words)*

This report discusses a transfer-matrix formalism for expressing the effect of a component on the mode-power distribution. It is expected this formalism will clarify and extend matrix approaches to the description of this effect presented by others and will result in component loss characterization methods that are independent of the launch conditions chosen to make the characterization.

The report shows that a reduced-dimension transfer matrix can be defined in terms of a rectangular matrix transformation from the full-dimension mode space to a reduced-dimension space and its pseudo-inverse. Further, it shows that the reduced-dimension space need not be a conventional mode-block partition. The report concludes that valid reduced-dimension representations should be attainable directly from vectorization of the near-field patterns without first developing the mode distribution.

14. SUBJECT TERMS		15. NUMBER OF PAGES
Transfer matrix Least-square-fit method	Near-field patterns	55
		16. PRICE CODE

17. SECURITY CLASSIFICATION OF REPORT	18. SECURITY CLASSIFICATION OF THIS PAGE	19. SECURITY CLASSIFICATION OF ABSTRACT	20. LIMITATION OF ABSTRACT
UNCLASSIFIED	UNCLASSIFIED	UNCLASSIFIED	UNLIMITED